Near-infrared transparent electrodes for precision Teng–Man electro-optic measurements: In_2O_3 thin-film electrodes with tunable near-infrared transparency

Lian Wang, Yu Yang, and Tobin J. Marks[a)]
Department of Chemistry and the Materials Research Center, Northwestern University, Evanston, Illinois 60208-3113

Zhifu Liu and Seng-Tiong Ho
Department of Electrical and Computer Engineering, and the Materials Research Center, Northwestern University, Evanston, Illinois 60208-3118

(Received 1 April 2005; accepted 15 August 2005; published online 13 October 2005)

Highly near-infrared (NIR) transparent In_2O_3 thin films have been grown by ion-assisted deposition at room temperature, and the optical and electrical properties characterized. NIR transparency and the plasma edge frequency can be engineered by control of the film deposition conditions. As-deposited In_2O_3 thin films were employed as transparent electrodes for direct thin film electro-optic (EO) characterization measurements via the Teng–Man technique. Using $LiNbO_3$ as the standard, the relationship between electrode NIR transparency and Teng–Man EO measurement accuracy was evaluated. It is found that In_2O_3 electrodes can be tailored to be highly NIR transparent, thus providing far more accurate Teng–Man EO coefficient quantification than tin-doped indium oxide. In addition, the EO coefficients of stilbazolium-based self-assembled superlattice thin films were directly determined for the first time using an optimized In_2O_3 electrode. EO coefficients r_{33} of 42.2, 13.1, and 6.4 pm/V are obtained at 633, 1064, and 1310 nm, respectively. © *2005 American Institute of Physics*. [DOI: 10.1063/1.2089184]

To date, the simple reflection technique developed by Teng and Man, is extensively used in characterization of the electro-optic (EO) properties of nonlinear optical (NLO) thin-film materials.[1] Here an EO-active film is sandwiched between a top transparent conducting electrode and a bottom metal electrode. This technique is extremely simple, convenient, in principle accurate, requires no waveguiding or cladding material, and is thus the preferred method for determining the EO coefficients (e.g., r_{33}) of NLO materials. Since the EO coefficient is typically wavelength dependent, direct EO coefficient measurement at different wavelengths, especially at telecommunication wavelengths (1310 and 1550 nm), is of great importance.

A primary assumption of the Teng–Man technique is that the laser beam passes through the EO film only twice—before and after reflection by the metal electrode. This requires high transmittance of the transparent electrode at the working wavelengths, otherwise the top electrode and metal electrode behave as a Fabry-Pérot resonator, giving rise to a systematic error in the measured EO coefficient. Transparent conducting oxide (TCO) thin films are usually used as top electrodes in Teng–Man measurements because they can be both optically transparent and electrically conductive. The most popular electrode material at present is tin-doped indium oxide (ITO).[2–4] ITO is a degenerate semiconductor with a carrier concentration of $\sim 10^{21}$ cm^{-3}. The optical transmittance of conventional (commercial) ITO exhibits a sharp plasma edge starting at wavelengths $\gtrsim 900$ nm due to free carrier scattering.[5] ITO electrodes therefore function well as top electrodes in the visible region, but are limited for measurements in the near-infrared (NIR) region.[4,6] Recently, Michelotti *et al.* reported that, compared to ITO, Al-doped ZnO exhibits improved Teng–Man accuracy at 1550 nm. However, to our knowledge, this particular material is far from optimum and introduces significant systematic error ($\sim 10\%$) arising from its limited NIR transparency.[4]

Ion-assisted deposition (IAD) is a unique thin-film growth technique which employs two ion beams to simultaneously effect film deposition, oxidation, and crystallization, resulting in smooth, adherent, and dense oxide thin films on various substrates at room temperature.[7] One important advantage of this technique is that In_2O_3 thin film microstructural, electrical, and optical properties can be finely tuned by the growth system O_2 partial pressure and ion beam energy during film growth. Moreover, IAD is capable of depositing high-quality TCO thin films on organic substrates at room temperature.[7]

In this letter, a series of highly NIR transparent In_2O_3 thin films is grown on glass substrates and single-crystal $LiNbO_3$, and evaluated as transparent electrodes for the Teng–Man technique. Here, $LiNbO_3$ with an accurately known r_{33},[8] is used as a standard, and the relationship between TCO electrode carrier concentration, NIR-transparency, and EO coefficient measurement accuracy is systematically investigated. The measurement accuracy is found to be strongly dependent on the degree of the NIR transparency. It is shown that In_2O_3 thin films with carrier concentrations in the range 10^{18}–$10^{19}$$cm^{-3}$ exhibit excellent NIR transparency (>90%), and provide far more accurate Teng–Man measurements than conventional ITO electrodes. In_2O_3 thin films were also successfully grown on organic self-assembled super-lattice (SAS) thin films for Teng–Man

[a)]Author to whom correspondence should be addressed; electronic mail: t-marks@northwestern.edu

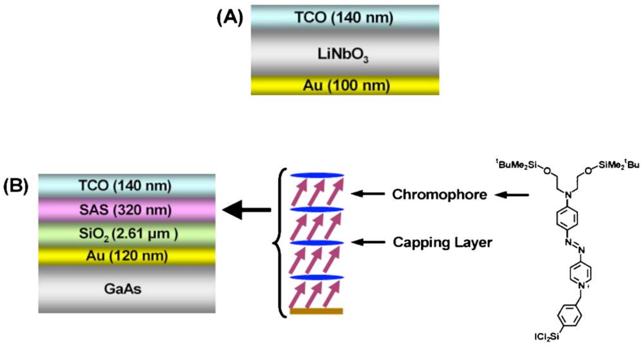

FIG. 1. (Color online) (A). Cross-sectional structure of a sandwiched $LiNbO_3$ Teng–Man sample. (B) Cross-sectional view of a SAS-based Teng–Man structure.

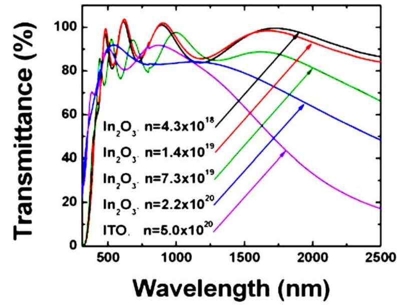

FIG. 2. (Color online) Transmission optical spectra and carrier concentrations of IAD-derived In_2O_3 and ITO thin films grown on 1737F glass substrates. The carrier concentrations and the thicknesses correspond to those for the samples in Table I.

measurements.[9] The EO coefficients are quantified at 633, 1064, and 1310 nm for the first time.

A series of In_2O_3 thin films with tunable NIR transparency was grown on Corning 1737F glass substrates using a Veeco horizontal dual-gun IAD system at room temperature. The O_2 partial pressure was maintained between $1.2\times10^{-4}-2.0\times10^{-4}$ Torr during film deposition. ITO was also deposited for comparison. In_2O_3 (99.99%) and ITO targets ($In_2O_3:SnO_2=9:1$) were purchased from Williams Advanced Materials and Sputtering Materials, Inc., respectively. In_2O_3 thin film growth rates were from 3–5 nm/min, depending on the conditions. Film thickness was measured with a Tencor P-10 step profilometer after etching a step in the film. Single-crystal $LiNbO_3$ slides (MTI Corp., Z cut, optical grade) were top coated with 140 nm In_2O_3 or ITO by room temperature IAD, and bottom coated with 100 nm gold by electron beam evaporation. The device structure $Au/LiNbO_3/In_2O_3$ or ITO is shown in Fig. 1(A). For organic SAS film samples, a 140 nm In_2O_3 electrode was deposited on the SAS films, which in turn were grown on a $SiO_2/Au/GaAs$ substrate using layer-by-layer self-assembly techniques. Details concerning SAS film growth are reported elsewhere.[9,10] The structure of the $In_2O_3/SAS/SiO_2/Au/GaAs$ specimen is shown in Fig. 1(B). A 633 nm He–Ne laser and 1064 and 1310 nm diode lasers were the laser sources. The frequency of the driving voltage applied to the samples was 1 KHz, and the amplitude ranged from 1 to 10 V.

The electrical properties of IAD-derived In_2O_3 thin films were characterized as a function of O_2 partial pressure (P_{O_2}) and primary ion beam energy (Table I). By increasing P_{O_2} and diminishing the primary ion beam energy, carrier In_2O_3 film concentrations can be incrementally reduced from 2.2×10^{20} to 4.3×10^{18} cm^{-3}, with conductivity dropping from 845 to 21 S/cm. It is known that In_2O_3 thin-film conductivity originates from oxygen vacancies or In^{3+} interstitials. With increasing P_{O_2}, more oxygen vacancies are compensated, leading to lower carrier concentrations and conductivities. Note that the decreased conductivity is caused by reduction in carrier concentration, not in mobility, which remains within a small range. Thus, the carrier concentrations and conductivities of In_2O_3 thin films are engineered by the IAD deposition conditions. ITO films with a conductivity of 1520 S/cm and a carrier concentration of 5.0×10^{20} cm^{-3} were obtained as reported previously.[7]

The optical transmittance spectra of In_2O_3 films as a function of carrier concentration are shown in Fig. 2. Note that the NIR transparency of the In_2O_3 thin films is a strong function of carrier concentration. The plasma edge progressively red-shifts as the film carrier concentration is decreased. When the concentration is $\leqslant1.4\times10^{19}$ cm^{-3}, the transmittance of In_2O_3 films with thickness ~450 nm is ~90% at 1310 nm and ~97% at 1550 nm, and there is no significant difference in transparency from the visible to NIR, indicating that free carrier scattering is not a dominant factor in NIR transparency. In contrast to the In_2O_3 films, the transmittance spectrum of ITO films, with a typical carrier concentration of 5×10^{20} cm^{-3} (Ref. 5), evidences a sharp plasma edge beginning at ~900 nm. The poor NIR transmittance is undoubtedly due to free carrier scattering at such high carrier concentrations, rendering ITO nonideal for NIR-sensitive measurements.

To evaluate In_2O_3 and ITO as transparent electrodes for Teng–Man measurements, and to investigate the relationship

TABLE I. Physical and electrical properties of IAD-derived In_2O_3 and ITO thin films.

Sample	Thickness (nm)	Sheet resistance (Ω/□)	Conductivity (S/cm)	Mobility (cm^2/V s)	Carrier concentration (cm^{-3})
1. In_2O_3	140	85	845	24	2.2×10^{20}
2. In_2O_3	150	108	631	28	1.4×10^{20}
3. In_2O_3	520	62	311	27	7.3×10^{19}
4. In_2O_3	450	342	65	29	1.4×10^{19}
5. In_2O_3	500	629	32	24	8.2×10^{18}
6. In_2O_3	450	1080	21	30	4.3×10^{18}
7. ITO	250	28	1520	19	5.0×10^{20}

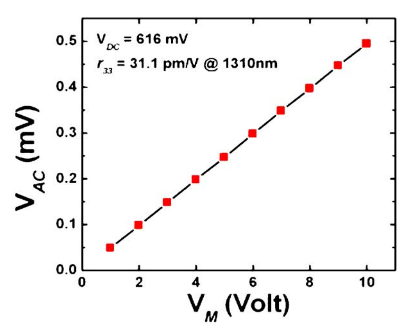

FIG. 3. (Color online) Modulated-beam signal V_{ac} vs applied voltage V_M recorded on an In_2O_3-coated $LiNbO_3$ Teng–Man specimen. This electrode corresponds to sample 1 in Table II.

TABLE II. Experimental r_{33} results for $LiNbO_3$ using 140 nm In_2O_3 and ITO electrodes in direct Teng–Man EO measurements at 1310 nm.

Sample	r_{33} (pm/V)	Relative deviation (%)	Electrode conductivity (S/cm)	Electrode carrier concentration (cm^{-3})
Standard value	30.8[a]			
1. In_2O_3	31.1	0.97	18	4.0×10^{18}
2. In_2O_3	29.5	−4.2	58	1.3×10^{19}
3. ITO	42.2	37.0	1400	4.5×10^{20}

[a]Standard value independently measured by the vendor, MTI Crystal Corporation.

between NIR transparency and Teng–Man measurement accuracy, Z-cut single-crystal $LiNbO_3$ was employed as a standard. The $Au/LiNbO_3/TCO$ structure [Fig. 1(A)] was used in this simple reflection configuration to evaluate the EO coefficient accuracy obtained with the different transparent electrodes. Here r_{33} is derived from Eq. (1)[2]

$$r_{33}=\frac{3\sqrt{2}}{4}\frac{\lambda}{\pi}\frac{1}{V_M}\frac{V_{ac}}{V_{dc}}\left[\frac{n_on_e\sin^2\theta}{\sqrt{n_e{}^2-\sin^2\theta}}+0.279\left(\frac{n_o{}^3}{n_e{}^2}\sqrt{n_e{}^2-\sin^2\theta}-\frac{n_o{}^4}{\sqrt{n^2-\sin^2\theta}}\right)\right], \tag{1}$$

where V_{dc} is the working voltage, V_{ac} is the modulated signal, V_M is the modulation voltage applied to the sample, θ is the incident angle of the laser beam (fixed at 45°), and n_o and n_e are the ordinary and extraordinary refractive indices of $LiNbO_3$, respectively. Experimental r_{33} determination results using In_2O_3 and ITO electrodes and electrical properties of the transparent electrodes, are summarized in Table II. The excellent linear relationship between modulated-beam signal V_{ac} and applied voltage V_M is displayed in Fig. 3. At 633 nm, both In_2O_3 and ITO electrodes exhibit good transparency and yield very close values of r_{33} vs the standard r_{33} value (30.8 pm/V). Likewise, r_{33} values measured using two different In_2O_3 electrodes are also in good agreement with the standard value, and their relative deviations being 0.97% and −4.2%, respectively (Table I). In contrast, r_{33} measured with the ITO electrode shows a very large deviation of +37.0% (Table I). Clearly, the accuracy of the derived r_{33} is strongly dependent on TCO electrode NIR transparency. The large deviation of the ITO-electrode derived r_{33} value presumably originates from reflection that leads to interference effects and Fabry-Pérot resonance, and hence introduces far greater error.[1,4] To maintain good experimental accuracy in the NIR region, the NIR transparency of the electrodes should be considered, and Teng–Man EO measurements may incur substantial inaccuracies using conventional ITO as the NIR transparent electrode, and the present In_2O_3 films provide excellent experimental accuracy. Considering the consistency in excellent transparency over the NIR region (Fig. 2), the present In_2O_3 electrodes should provide high accuracy at 1550 nm or further into the NIR.

Teng–Man measurements were next carried out on intrinsically polar SAS thin films using optimized In_2O_3 electrodes. SAS thin films have been used for fabrication of EO phase modulators.[10] Direct EO measurements on SAS films were carried as for $LiNbO_3$ films, with a 140 nm high-quality In_2O_3 film deposited by IAD on the SAS films at room temperature. The In_2O_3 thin-film conductivity and carrier concentration were 24 S/cm and 4.2×10^{18} cm^{-3}, respectively. Assuming $r_{33}=3r_{13}$ and using the approximation $n_o\approx n_e\approx n$, Eq. (1) simplifies to Eq. (2) for SAS thin films

$$r_{33}=\frac{3\sqrt{2}}{4}\frac{\lambda}{\pi}\frac{1}{V_M}\frac{V_{ac}}{V_{dc}}\frac{\sqrt{n_{SAS}^2-\sin^2\theta}}{n_{SAS}^2\sin^2\theta}. \tag{2}$$

The highest r_{33} determined is 42.2 pm/V at 633 nm. At 1064 nm, r_{33} becomes 13.1 pm/V agreeing well with waveguiding EO modulator measurements.[10] An r_{33} of 6.4 pm/V is obtained at 1310 nm, indicating that the EO response of SAS thin films exhibits a pronounced dispersion with wavelength.[11–13] These SAS results further demonstrate the effectiveness of In_2O_3 electrodes for direct EO measurements.

In summary, highly NIR transparent In_2O_3 thin films grown on glass substrates, single-crystal Z-cut $LiNbO_3$, and organic SAS thin films by room temperature IAD, can be employed as transparent electrodes for precision Teng–Man EO measurements. Tunable NIR transparency can be achieved by controlling the carrier concentration. It is found that Teng–Man measurement accuracy strongly depends on the NIR transparency of the TCO electrodes. In addition, the suitability of IAD-In_2O_3 electrodes was further demonstrated by characterizing the EO properties of organic SAS thin films. Importantly, highly NIR transparent In_2O_3 films should have many other applications in NIR-sensitive optoelectronic devices and measurements.

The authors thank DARPA/ONR (N00014-04-1-0093/P0001) and the NSF-MRSEC program through the Northwestern Materials Research Center (DMR-0076097) for support of this research.

[1]C. C. Teng and H. T. Man, Appl. Phys. Lett. **56**, 1734 (1990).
[2]Y. Shuto and M. Amano, J. Appl. Phys. **77**, 4632 (1995).
[3]J. S. Schildkraut, Appl. Opt. **29**, 2839 (1990).
[4]F. Michelotti, A. Belardini, M. C. Larciprete, M. Bertolotti, A. Rousseau, A. Ratsimihety, G. Schoer, and J. Mueller, Appl. Phys. Lett. **83**, 4477 (2003).
[5]H. L. Hartnagel, A. L. Dawar, A. K. Jain, and C. Jagadish, *Semiconducting Transparent Thin Films* (IOP, 1995), p. 273.
[6]P. A. Chollet, G. Gadret, F. Kajzar, and P. Raimond, Thin Solid Films **242**, 132 (1994).
[7]Y. Yang, Q. L. Huang, A. W. Metz, J. Ni, S. Jin, T. J. Marks, M. E. Madsen, A. DiVenere, and S. T. Ho, Adv. Mater. (Weinheim, Germany) **16**, 321 (2004).
[8]The standard value is independently measured by MTI Crystal Corporation.
[9]P. W. Zhu, M. E. van der Boom, H. Kang, G. Evmenenko, P. Dutta, and T. J. Marks, Chem. Mater. **14**, 4982 (2002).
[10]S. T. Ho, Z. Liu, J. Ma, G. Xu, B. Liu, T. J. Marks, P. W. Zhu, H. Kang, and A. Facchetti, *Proc. GOMACTech-04* 2005, p. 231.
[11]S. Kalluri, S. Garner, M. Ziari, W. H. Steier, Y. Shi, and L. R. Dalton, Appl. Phys. Lett. **69**, 275 (1996).
[12]H. S. Nalwa and S. Miyata, *Nonlinear Optics of Organic Molecules and Polymers* (CRC, Boca Raton, FL, 1996), p 397.
[13]P. M. Lundquist, W. Lin, H. Zhou, D. N. Hahn, S. Yitzchaik, T. J. Marks, and G. K. Wong, Appl. Phys. Lett. **70**, 1941 (1997).